



ISSN: 2076-5061

Photocatalytic decolorization of methyl orange dye using SnO₂-TiO₂ nanocomposite particles synthesised by Ultrasonic Assisted Co-Precipitation Method

Md. Abdus Samad Azad^{1*}, Newaz Muhammed Bahadur¹,
Md Shahadat Hossain², Abdullah Al Masum³

¹Department of Applied Chemistry and Chemical Engineering, Noakhali Science and Technology University, Sonapur, Noakhali-3814, Bangladesh, ²Department of Innovation Systems Engineering, Graduate School of Engineering, Utsunomiya University, 7-1-2 Yoto, Utsunomiya 321-8585, Japan, ³Faculte de Science, Université Paris-Saclay, 91405 Orsay cedex, France

ABSTRACT

The ultrasonic-aided co-precipitation method was used to create SnO₂-TiO₂ nanocomposite particles. Scanning electron microscopy (SEM), X-ray diffraction (XRD), Fourier transform infrared spectroscopy (FT-IR), and UV-vis spectroscopy were used to characterize the nanocomposite particles. XRD patterns revealed the crystalline structure of particles and the average particle size determined by Debye Scherrer's equation was found to be 11.355, 4.9577, and 4.333 nm for TiO₂ nanoparticles, SnO₂ nanoparticles, and SnO₂-TiO₂ nanocomposites, respectively. The Ti, Sn, and O species were confirmed to exist by energy-dispersive X-ray spectroscopy (EDS). The UV absorption peaks at 288, 305, and 350 nm were attributed to SnO₂, TiO₂-SnO₂, and TiO₂ respectively. The photocatalytic aspect was investigated in a model organic contaminant (methyl orange). Data obtained by the above-mentioned characterization methods confirmed the superior photocatalytic activity of SnO₂-TiO₂ nanostructure than SnO₂ or TiO₂ alone.

KEYWORDS: TiO₂, SnO₂, Ultrasonic irradiation, Nanocomposite, Photocatalytic activity

Received: January 07, 2023
Revised: March 14, 2023
Accepted: March 16, 2023
Published: March 24, 2023

*Corresponding Author:
Md. Abdus Samad Azad
E-mail: samad.acce@nstu.edu.bd

INTRODUCTION

Various organic and inorganic pollutants released without treatment by some industries, especially textile industries lead to public health concerns and endanger the aquatic ecosystem (Bahadur *et al.*, 2019). Unfortunately, In spite of being carcinogenic & mutagen, over 50,000 tons of untreated effluent are added per annum (Beltrán-Heredia *et al.*, 2009).

Toxicity, non-biodegradability, and stability in aquatic medium make azo dye one of the most notorious classes among the synthetic dyes that are frequently found in industrial wastewater (Ventura-Camargo & Marin-Morales, 2013). To avoid the issues outlined above, it is essential that these harmful species are eliminated from industrial wastewater.

For the treatment of industrial wastewater, a number of techniques are frequently used, including adsorption (Zhu

et al., 2014), flocculation-precipitation (Yang *et al.*, 2013), membrane filtration (Liang *et al.*, 2014), ozonation (Li & Yeung, 2019), and electrochemical methods (Ltaïef *et al.*, 2018), & so on. Photocatalysis is one of the promising techniques for dye degradation using semiconductors as catalysts under light irradiation, and extensive research has been ongoing for wastewater treatment following the photocatalytic method (Negishi *et al.*, 2019). Photocatalysts of different varieties such as ZnO, TiO₂, Al₂O₃, Fe₃O₄, WO₃, and CeO₂, as well as their composites have been investigated to utilize their unique property for the degradation purpose (organic contaminant) (Munir *et al.*, 2015).

The most promising photocatalyst has been thought to be TiO₂, even though several nanoparticles exhibit photocatalytic activity. Thanks to its strong photocatalytic activity, chemical and physical stability, lack of toxicity, low price, and ease of availability (Indris *et al.*, 2005; Liu *et al.*, 2009). Although several advancements have been achieved, photoinduced electron-hole

Copyright: © The authors. This article is open access and licensed under the terms of the Creative Commons Attribution License (<http://creativecommons.org/licenses/by/4.0/>) which permits unrestricted, use, distribution and reproduction in any medium, or format for any purpose, even commercially provided the work is properly cited. Attribution — You must give appropriate credit, provide a link to the license, and indicate if changes were made.

pairs with shorter lifetime makes it inappropriate for large-scale use. One possible solution for the fast annihilation of charge carriers is sensitizing the TiO_2 with metals and narrow band gap semiconductors by adopting a strategy of band gap modification. The electron & hole annihilation rate of TiO_2 photocatalysts can be slowed down by a narrow band gap semiconductor or metal which is to be a sink or electron trap (Zhou *et al.*, 2010).

Tin (IV) Oxide (SnO_2) is a well-known metal oxide whose major charge carrier is electron (n-type) and considerably transparent ($\sim 80\%$) in wavelengths of visible spectra. Its crystal structure is rutile structure and can be synthesized of distinct nano-structure following different cost efficient synthesis methods which are applicable in different fields such as sensing devices, flat panel displays, photovoltaic devices, etc (Singh & Nakate, 2013).

In this work, TiO_2 , SnO_2 , and $\text{SnO}_2\text{-TiO}_2$ have been prepared by a simple, cost-effective, and environment-friendly ultrasonic-assisted co-precipitation method. The findings of the present work illustrated an improved photo-degradation efficacy of $\text{SnO}_2\text{-TiO}_2$.

EXPERIMENTAL DETAILS

Synthesis of SnO_2 Nanoparticles

Without additional purification, aqueous ammonia was utilized as the precipitant with $\text{SnCl}_4 \cdot 5\text{H}_2\text{O}$ as the starting material. The aqueous ammonia solution was added dropwise to the rapidly stirred mixed solution after dissolving $\text{SnCl}_4 \cdot 5\text{H}_2\text{O}$ in a small volume of deionized water. The pH of the solution was then adjusted to around 7, and a substantial amount of white slurry was produced. The resultant slurry was centrifuged for 10 minutes at 7000 rpm after being continuously sonicated for 2 hours. To create the SnO_2 photocatalyst, the residue was first dried in air at a temperature of around 105°C , and then it was cleaned three times with ethanol.

Synthesis of TiO_2 Nanoparticles

100 mL of ethanol and 1.43 mL of deionized water were combined with 1 mL of TBOT. After that, a magnetic stirrer was used to mix it for 10 minutes. The resulting mixture was ultrasonically irradiated for 4 hours at room temperature, followed by a 10-minute centrifugation at 7000 rpm. The residue was dried at 120°C for five hours after being rinsed three times with ethanol.

Preparation of $\text{SnO}_2\text{-TiO}_2$ Nanocomposite Particles

The co-precipitation method with ultrasonic assistance was used to create $\text{SnO}_2\text{-TiO}_2$. 3.65 grams of $\text{SnCl}_4 \cdot 5\text{H}_2\text{O}$ were dissolved in 100 mL of deionized water in a beaker. In a different beaker, 4 mL of TBOT, 100 mL of ethanol, and 1.43 mL of deionized water were combined and swirled for 10 minutes. After rapidly stirring the TBOT solution, the produced SnO_2 solution was added. The pH of the mixture was then adjusted to (7) by adding aqueous ammonia. To create the nanocomposite particles, the white slurry created in the previous step was first centrifuged at

7500 rpm for 10 minutes, then washed three times with ethanol before being dried in the air at roughly 105°C for 24 hours.

RESULTS AND DISCUSSION

Optical Properties

Figure 1 displays the SnO_2 , TiO_2 , and $\text{SnO}_2\text{-TiO}_2$ nanoparticles' UV-vis absorption spectra. While TiO_2 particles displayed an optical absorption at 350 nm and the SnO_2 showed an absorption peak at 288 nm, the sharp peak at 288 nm is the typical absorption peak of SnO_2 (Swarnkar *et al.*, 2011). At 305 nm, the $\text{SnO}_2\text{-TiO}_2$ displayed optical absorption (Yu *et al.*, 2002; Sridhar & Sriharan, 2014).

Structural Analysis

X-ray Diffraction (XRD) was used to examine the phase structures and particle size distribution of pure TiO_2 , SnO_2 , and $\text{SnO}_2\text{-TiO}_2$ nanomaterials heat treated at 500°C . The XRD patterns of (a) $\text{SnO}_2\text{-TiO}_2$ nanoparticles and (b) TiO_2 and SnO_2 nanoparticles are displayed in Figure 2.

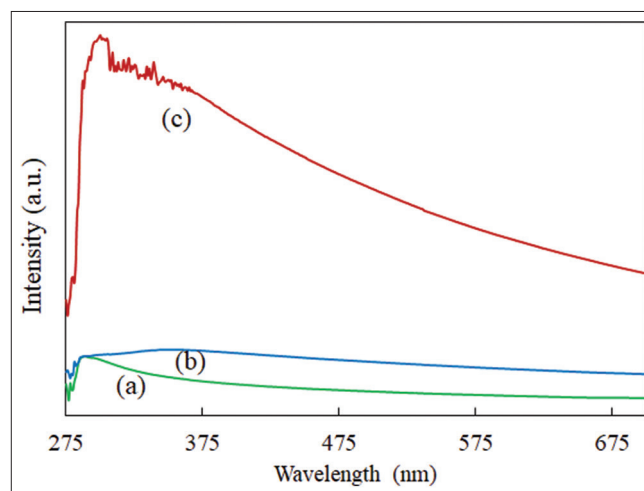


Figure 1: UV-visible absorption spectra of (a) pure SnO_2 nanoparticles, (b) pure TiO_2 nanoparticles, and (c) $\text{SnO}_2\text{-TiO}_2$ nanoparticles

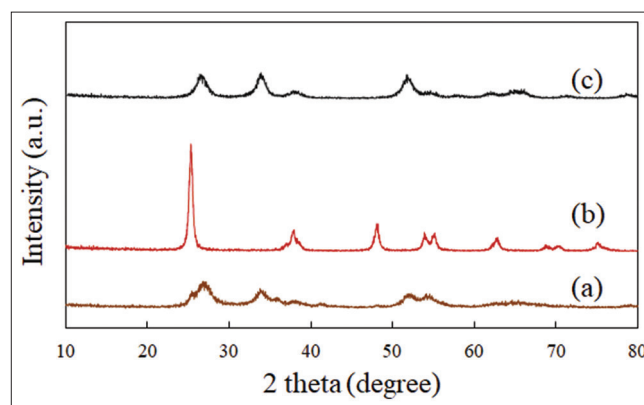


Figure 2: X-ray diffraction patterns of (a) $\text{SnO}_2\text{-TiO}_2$ nanocomposite particles (annealed at 500°C), (b) pure TiO_2 nanoparticles, and (c) pure SnO_2 nanoparticles

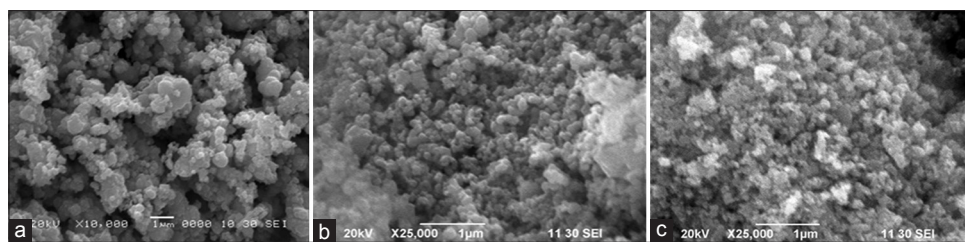


Figure 3: FE-SEM images of (a) pure SnO₂ nanoparticle, (b) pure TiO₂ nanoparticles, and (c) SnO₂-TiO₂ nanocomposite particles.

The creation of the SnO₂-TiO₂, TiO₂, and SnO₂ crystal formations is evident in the XRD pattern.

Using Debye Scherrer's equation, the average crystallite size, *d* in the SnO₂, TiO₂, and SnO₂-TiO₂ is derived from the observed full width at half maximum (FWHM) values of the XRD peaks (Zhou & Wu, 2001).

$$d = \frac{0.89\lambda}{\beta \cos\theta}$$

Where *d* is the calibrated FWHM of the chosen diffraction peak, θ is the Bragg's diffraction angle, and λ is the wavelength of the X-ray source. SnO₂, TiO₂, and SnO₂-TiO₂ nanoparticles' typical crystallographic sizes have been determined to be 4.96, 11.36, and 4.33 nm, respectively.

Morphological Studies

The surface morphology of the SnO₂, TiO₂ and SnO₂-TiO₂ nanoparticles was investigated by SEM analysis. Figure 3 shows the typical SEM images of (a) SnO₂, (b) TiO₂ and (c) SnO₂-TiO₂ nanoparticles. From the SEM image, it can be seen that the particles are spherical-shaped and the size of most of the particles is less than 50 nm. SnO₂ and TiO₂ particles were well distributed, but the surface morphology had changed in the SnO₂-TiO₂. In the SEM image of SnO₂-TiO₂ SnO₂ represents brighter particles due to the higher electron density of SnO₂ to TiO₂ and darker particles represent TiO₂. The surfaces of the SnO₂-TiO₂ are rough and textured, indicating that SnO₂ particles were widely dispersed on the TiO₂, which would be beneficial to improve the photocatalytic activity.

Energy-dispersive X-ray spectrum (EDS) of SnO₂-TiO₂ is shown in Figure 4. It indicates that the nanoparticles are only composed of Ti, Sn and O elements and no other elements. The results of the EDS analysis were in good agreement with the above results. The mass and atomic percentage of Sn, Ti, and O in SnO₂-TiO₂ are shown in Table 1.

Photocatalytic Degradation Studies

The photocatalytic efficiency of TiO₂, SnO₂ & SnO₂-TiO₂ nanoparticles was investigated by measuring the photocatalyzed discoloration rate of Methyl Orange in an aqueous solution. Five bulbs (22-inch, 15 W) with the strongest band at the wavelength of 352 nm were used as the UV-irradiation source. An aqueous solution of MO (5.00 × 10⁻⁵ M) and the photocatalyst (0.2 g) were placed in a Pyrex beaker and the

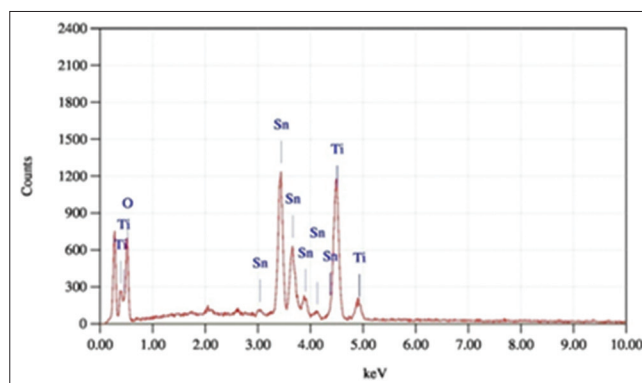


Figure 4: EDS spectra of SnO₂-TiO₂ nanocomposite particles

Table 1: Elemental analysis of SnO₂-TiO₂ sample using EDS analysis

Element	Mass (%)	Error Mass (%)	Atom Mass (%)
O	6.69	0.02	26.68
Ti	29.10	0.02	38.78
Sn	64.22	0.02	34.54
Total	100.00		100.00

particles were kept in suspension at the dark with 400 rpm magnetic stirring for 30 min to ensure adsorption/desorption equilibrium and then the mixture was UV irradiated. After given intervals of UV irradiation, a small amount of the suspension was collected and centrifuged at 10000 rpm for 10 min to remove the catalyst, and the remaining MO solution was characterized with UV-visible spectroscopy. The intensity drop in the characteristic peak of MO at 467 nm was used as the basis for the photocatalytic efficiency of the composite particles. The following equation was used to quantify the photocatalytic degradation frequency of MO aqueous medium.

$$D = \frac{C_0 - C}{C_0} \times 100 = \frac{A_0 - A}{A_0} \times 100$$

where *D* represents the photocatalytic degradation rate of MO (Methyl Orange) solution, *C*₀ and *C* are the pre & post-irradiation concentration of the dye; *A*₀ and *A* are the pre & post-irradiation absorbance of MO solution at 463nm as measured by the UV-Vis spectrophotometer, respectively.

Figure 5 shows the photocatalytic degradation percentage of MO using SnO₂, TiO₂ and SnO₂-TiO₂ as the catalyst. After 6 hours, the photocatalytic degradation rate of MO was calculated as 58% and 81% when SnO₂ and TiO₂ were used as the catalyst.

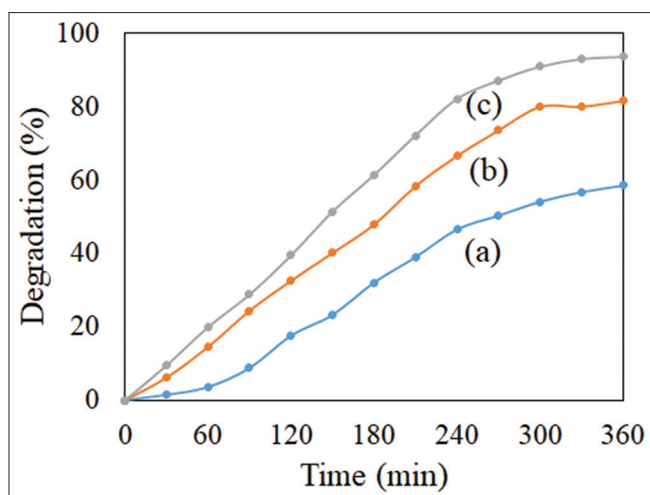


Figure 5: Photocatalytic degradation rate of MO using (a) SnO₂, (b) TiO₂, and (c) SnO₂-TiO₂ as the catalyst

On the other hand, 93% of degradation was achieved using SnO₂-TiO₂.

CONCLUSIONS

SnO₂, TiO₂ and SnO₂-TiO₂ have been prepared in a crystalline form, by a simple and fast ultrasound-assisted co-precipitation method. XRD and EDS analysis confirmed the successful doping of SnO₂ and TiO₂ in the SnO₂-TiO₂. SEM images revealed the bright spots of SnO₂ in SnO₂-TiO₂ due to the high electron density of SnO₂. SnO₂-TiO₂ revealed high photocatalytic activity as compared to SnO₂ and TiO₂. Approximately 93% degradation of Methyl Orange (MO) dye was reported by using SnO₂-TiO₂ in 6 hours, while only 58% and 81% degradation was achieved using SnO₂ and TiO₂, respectively at the same time. Our next plan is to implement this research work in antimicrobial work and use stannic oxide particles in gas sensing to remove pollutants from the environment, to clean our environment and our planet. To live a healthy life, it is mandatory to keep our environment clean, pollutant-free and healthy.

ACKNOWLEDGEMENT

The Ministry of Science and Technology (MOST) of Bangladesh and the University Grant Commission (UGC) of Bangladesh provided financial assistance for this research.

REFERENCES

Bahadur, N. M., Chowdhury, F., Obaidullah, M., Hossain, M. S., Rashid, R., Akter, Y., Furusawa, T., Sato, M., & Suzuki, N. (2019). Ultrasonic-assisted synthesis, characterization, and photocatalytic application of SiO₂@TiO₂ core-shell nanocomposite particles. *Journal of Nanomaterials*, 2019, 6368789. <https://doi.org/10.1155/2019/6368789>

Beltrán-Heredia, J., Sánchez-Martín, J., & Delgado-Regalado, A. (2009). Removal of carmine indigo dye with *Moringa oleifera* seed extract.

Industrial & Engineering Chemistry Research, 48(14), 6512-6520. <https://doi.org/10.1021/ie9004833>

Indris, S., Amade, R., Heitjans, P., Finger, M., Haeger, A., Hesse, D., Grünert, W., Börger, A., & Becker, K. D. (2005). Preparation by high-energy milling, characterization, and catalytic properties of nanocrystalline TiO₂. *The Journal of Physical Chemistry B*, 109(49), 23274-23278. <https://doi.org/10.1021/jp054586t>

Li, Y., & Yeung, K. L. (2019). Polymeric catalytic membrane for ozone treatment of DEET in water. *Catalysis Today*, 331, 53-59. <https://doi.org/10.1016/j.cattod.2018.06.005>

Liang, C.-Z., Sun, S.-P., Li, F.-Y., Ong, Y.-K., & Chung, T.-S. (2014). Treatment of highly concentrated wastewater containing multiple synthetic dyes by a combined process of coagulation/flocculation and nanofiltration. *Journal of Membrane Science*, 469, 306-315. <https://doi.org/10.1016/j.memsci.2014.06.057>

Liu, P., Cai, W., Fang, M., Li, Z., Zeng, H., Hu, J., Luo, X., & Jing, W. (2009). Room temperature synthesized rutile TiO₂ nanoparticles induced by laser ablation in liquid and their photocatalytic activity. *Nanotechnology*, 20(28), 285707. <https://doi.org/10.1088/0957-4484/20/28/285707>

Ltaïef, A. H., Sabatino, S., Proietto, F., Ammar, S., Gadri, A., Galia, A., & Scialdone, O. (2018). Electrochemical treatment of aqueous solutions of organic pollutants by electro-Fenton with natural heterogeneous catalysts under pressure using Ti/IrO₂-Ta₂O₅ or BDD anodes. *Chemosphere*, 202, 111-118. <https://doi.org/10.1016/j.chemosphere.2018.03.061>

Munir, S., Dionysiou, D. D., Khan, S. B., Shah, S. M., Adhikari, B., & Shah, A. (2015). Development of photocatalysts for selective and efficient organic transformations. *Journal of Photochemistry and Photobiology B: Biology*, 148, 209-222. <https://doi.org/10.1016/j.jphotobiol.2015.04.020>

Negishi, N., Miyazaki, Y., Kato, S., & Yang, Y. (2019). Effect of HCO₃⁻ concentration in groundwater on TiO₂ photocatalytic water purification. *Applied Catalysis B: Environmental*, 242, 449-459. <https://doi.org/10.1016/j.apcatb.2018.10.022>

Singh, A. K., & Nakate, U. T. (2013). Microwave synthesis, characterization and photocatalytic properties of SnO₂ nanoparticles. *Advances in Nanoparticles*, 2, 66-70. <https://doi.org/10.4236/anp.2013.21012>

Sridhar, D., & Sriharan, N. (2014). Structural, Morphological and Optical Features Of SnO₂ and Cu₂O Doped TiO₂ Nanocomposites Prepared by Sol-Gel Method. *Journal of Nanoscience and Nanotechnology*, 2(1), 94-98.

Swarnkar, R. K., Singh, S. C., & Gopal, R. (2011). Effect of aging on copper nanoparticles synthesized by pulsed laser ablation in water: structural and optical characterizations. *Bulletin of Materials Science*, 34(7), 1363-1369.

Ventura-Camargo, B. de C., & Marin-Morales, M. A. (2013). Azo dyes: characterization and toxicity-a review. *Textiles and Light Industrial Science and Technology*, 2(2), 85-103.

Yang, Z., Yang, H., Jiang, Z., Cai, T., Li, H., Li, H., Li, A., & Cheng, R. (2013). Flocculation of both anionic and cationic dyes in aqueous solutions by the amphoteric grafting flocculant carboxymethyl chitosan-graft-polyacrylamide. *Journal of Hazardous Materials*, 254-255, 36-45. <https://doi.org/10.1016/j.jhazmat.2013.03.053>

Yu, J., Yu, J. C., Cheng, B., & Zhao, X. (2002). Photocatalytic activity and characterization of the sol-gel derived Pb-doped TiO₂ thin films. *Journal of Sol-Gel Science and Technology*, 24, 39-48. <https://doi.org/10.1023/A:1015109515825>

Zhou, W., Liu, H., Wang, J., Liu, D., Du, G., & Cui, J. (2010). Ag₂O/TiO₂ nanobelts heterostructure with enhanced ultraviolet and visible photocatalytic activity. *ACS Applied Materials & Interfaces*, 2(8), 2385-2392. <https://doi.org/10.1021/am100394x>

Zhou, Y., & Wu, G. H. (2001). *Material Analysis and Test Technique-XRD and Electronic Macroscopic Analysis of Material*. Harbin, China: Harbin Institute of Technology press.

Zhu, X., Liu, Y., Zhou, C., Zhang, S., & Chen, J. (2014). Novel and high-performance magnetic carbon composite prepared from waste hydrochar for dye removal. *ACS Sustainable Chemistry & Engineering*, 2(4), 969-977. <https://doi.org/10.1021/sc400547y>